

# Applications and equivalent models for coupled inductor parallel interleaved converters.

David Finn, Geoff Walker, Paul Sernia, Jordan Pierce.

School of Information Technology and Electrical Engineering

The University of Queensland, St Lucia, QLD 4072, Australia.

Email: dfinn@itee.uq.edu.au

## Abstract

Parallel interleaved converters are finding more applications everyday, for example they are frequently used for VRMs on PC main boards mainly to obtain better transient response.

Parallel interleaved converters can have their inductances uncoupled, directly coupled or inversely coupled, all of which have different applications with associated advantages and disadvantages. Coupled systems offer more control over converter features, such as ripple currents, inductance volume and transient response. To be able to gain an intuitive understanding of which type of parallel interleaved converter, what amount of coupling, what number of levels and how much inductance should be used for different applications a simple equivalent model is needed. As all phases of an interleaved converter are supposed to be identical, the equivalent model is nothing more than a separate inductance which is common to all phases. Without utilising this simplification the design of a coupled system is quite daunting.

Being able to design a coupled system involves solving and understanding the RMS currents of the input, individual phase (or cell) and output. A procedure using this equivalent model and a small amount of modulo arithmetic is detailed.

## I. Introduction

Uncoupled parallel interleaved converters are enjoying wide acceptance in applications that require high current, low voltage and fast transient response. One of the major applications is voltage regulator modules (VRMs) for processor power supplies.

An interleaved converter is beneficial in any application requiring a faster transient response without increasing steady state output current ripple or requiring mass and volume minimisation.

In these applications or others that already use interleaved converters coupling their output inductances allows for independent control over the cell and output ripple currents as well as the possibility for further improvement of the transient response.

The effects of coupling output inductances of interleaved converters have previously been considered in [1], [2], [3], [4], [5] with some equivalent models presented in [2]. A novel contribution of this paper is the addition of an equivalent voltage source to the equivalent model. The paper also presents unique procedure for calculating steady state current ripple, allowing RMS currents for input, cell and output to be calculated by hand with minimal effort. Using this procedure leads to a greater understanding of the operation of coupled systems.

The possible physical structures of the magnetics for a parallel interleaved converter are shown in Figure 1. Figure 1(a) shows the uncoupled case where no flux paths are shared. All the MMFs are in series for direct coupling, shown in Figure 1(b). All the MMFs are in parallel for indirect coupling, shown in Figure 1(c).

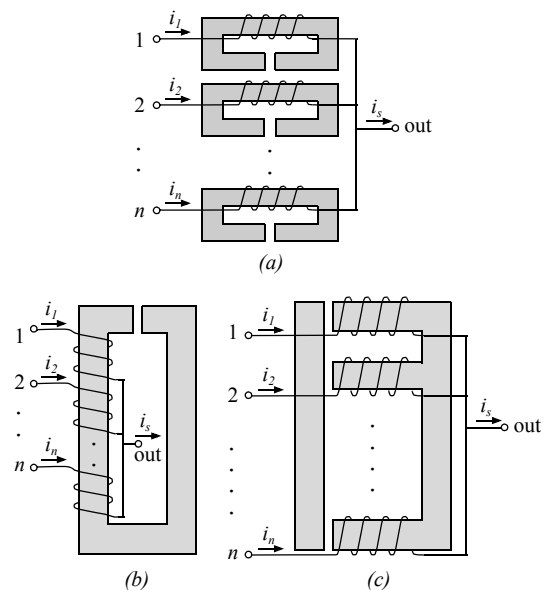


Figure 1 - Magnetic configurations for (a) Uncoupled, (b) Directly Coupled and (c) Inversely Coupled.

## II. Equivalent Model

To be able to intuitively understand the effects of changing inductance, coupling factor, number of levels and coupling polarity of a coupled inductor system an equivalent model is needed. Additionally, an equivalent model can be used to calculate the input, cell and output RMS currents, which are needed to be able to design a parallel interleaved converter.

Without an equivalent model the coupled inductor matrix equation (1) or a simulation package such as PSpice has to be used to solve for the cell currents and hence the input and output currents. These methods do not, however, help in understanding the sensitivity of voltages and current to design parameters. Like any simulation tools, these methods are better used to fine tune a design.

$$\begin{pmatrix} V_1 \\ V_2 \\ \vdots \\ V_n \end{pmatrix} = \begin{pmatrix} L_{11} & M_{12} & \cdots & M_{1n} \\ M_{12} & L_{22} & \cdots & M_{2n} \\ \vdots & \vdots & \ddots & \vdots \\ M_{1n} & M_{2n} & \cdots & L_{nn} \end{pmatrix} \begin{pmatrix} i_1 \\ i_2 \\ \vdots \\ i_n \end{pmatrix} \quad (1)$$

where self inductance is  $L_{ii} = \frac{N_i^2}{\mathfrak{R}_i}$   
and mutual inductance is  $M_{ij} = \frac{N_i N_j}{\mathfrak{R}_{ij}}$

If it is assumed of equation (1) that the  $L$ 's are all equal and the  $M$ 's are also all equal then the inductive filter, which is shown in Figure 2, models the function of equation (1) exactly. It is desired in this application for all the cells to operate in the same manner with the same ripple, therefore any deviation in inductances and coupling factors between cells is purely related to the practicality of physical construction of these magnetic structures. Optimising the design to account for these deviations is best done with Spice or similar simulation package.

The values for  $L$  and  $M$  for uncoupled, directly coupled and inversely coupled inductor systems are given in Table 1. They are given in terms of leakage inductance,  $L_L$ , and magnetising inductance,  $L_m$ .

Type of Coupling	Self Inductance ( $L$ )	Mutual Inductance ( $M$ )
Uncoupled	$L$	$0$
Direct	$L_L + L_m$	$L_m$
Inverse	$L_L + L_m$	$-L_m / (n-1)$ [eq.(23)]

Table 1 - Values for  $L$  and  $M$  in equation (1).

The values in Table 1 for uncoupled and directly coupled are fairly obvious. The value of mutual inductance for the inversely coupled case is obvious for the 2-cell case where it would equal  $-L_{mag}$ , but not so obvious for a  $n$ -cell converter. This inductance is derived in the Appendix of this paper, with the result given as equation (23).

The  $n$ -level parallel interleaved converter shown in Figure 2 shows the split between cell and output inductance, the derivation of these cell inductance and output inductance is shown in the Appendix, section B.

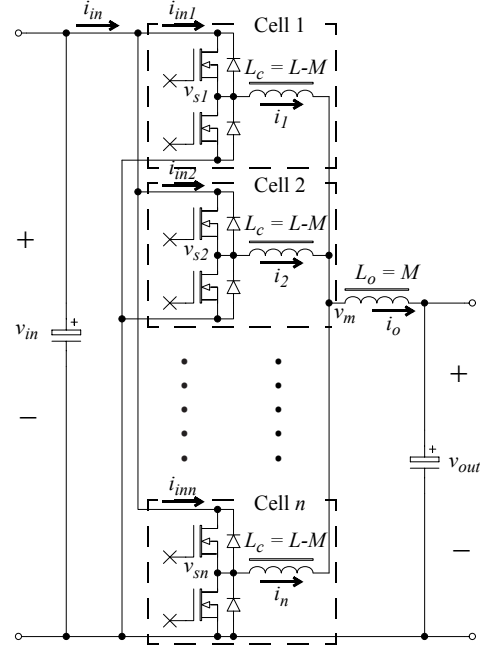


Figure 2 - A schematic of  $(n+1)$ -level parallel interleaved converter with equivalent inductive filter.

The multilevel equivalent input voltage and the equivalent output inductance of the complete interleaved switching circuit is shown in Figure 3. The derivation of this circuit from equation (1) can be found in the Appendix, section A. The input voltage to the left of Figure 3 produces exactly the same voltage waveforms as a interleaved series multilevel converter. Like any other multilevel system with interleaving the effective switching frequency of the new input voltage source is now  $n$  times faster than a single cell converter. Given that a parallel interleaved converter produces exactly the same multiple voltage levels through voltage averaging as a multilevel converter, it seems legitimate to refer to parallel interleaved converters as multilevel converters.

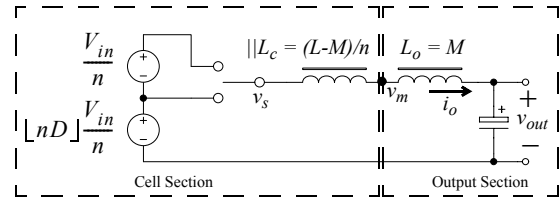


Figure 3 - Equivalent output circuit.

### A. Uncoupled

Although this case is fairly widely used and understood, a recap of the operation and benefits of uncoupled parallel interleaving will be given. This is

needed as a comparison to the coupled cases, which are also interleaved and hence also experience all the benefits of an uncoupled converter.

As can be seen from Figure 3 a parallel interleaved converter can be considered as a multilevel converter. Comparing a  $(n+1)$ -level converter to a simple 2-level converter with an inductance of  $L$ . A  $(n+1)$ -level converter will only ever apply one  $n$ th the voltage to the equivalent output inductance. As well, the interleaving effectively increases the switching frequency by a factor of  $n$ . Given the PWM voltage steps are one  $n$ th the size and the effective PWM frequency is  $n$  times faster the individual inductances can be reduced to  $L/n$  without changing the output ripple current. This gives an effective output inductance of  $L/n^2$ , which allows a  $n^2$  faster transient response.

This fast transient response is the reason why parallel interleaved converters are being used as VRMs for the latest processors.

The disadvantage of such a system is the increase in cell ripple current and hence RMS losses. In the comparison given above the cell current ripple will be  $n$  time larger and the average cell current will be  $n$  times smaller than the 2-level converter case. This means that as a percentage of the average cell current the cell current ripple has increased  $n^2$  times. Even if the cell inductances were left as  $L$  the current ripple would not have increased, but average cell current would have still decreased by  $n$  times meaning the percent ripple would be increased  $n$  times. This increase in ripple current can be thought of as a magnetising current in a transformer.

### **B. Direct coupling**

Firstly it can be seen how direct coupling is no different at all in terms of filtering than simply adding separate output inductance. In terms of loss, the separate output inductance will have less loss than the directly coupled solution. This is because the large cell ripple currents that exists in the small leakage inductances  $L_l$  would also exist in the multiple windings of the magnetising inductance  $L_m$ .

Although the concept of direct coupling is not necessarily advantageous, it should be noted that as inductance is shifted from the leakage to the common output inductance the cell current ripple continues to increase as the output ripple decreases. However, this is at the expense of transient response. Increasing cell current ripple seems wrong, but if it is increased enough, the current in each cell can actually be made to go negative and hence clamped zero voltage switching can now be achieved.

It can also be shown that, for the same amount of core and copper volume, one large inductor has square root  $n$  times more inductance than  $n$  paralleled inductors all with  $1/n$  the current rating. This means that

for the same core and copper volume, the current ripple can almost be reduced by square root  $n$  on an uncoupled case.

Once zero voltage switching is achieved, the switching frequency can now be increased quite substantially and either the output ripple current is reduced or inductance reduced and hence fast transient response and/or lower mass and volume.

Clamped zero voltage switching means that the switching frequency is now inversely proportional to the average output current. So, the ripple at low currents will have to be allowed to increase above  $2I_o/n$ .

### **C. Inversely coupling**

Inversely coupling does create a structure that can not be achieved in any other fashion. Inversely coupled interleaved converters have a negative output inductance. This inductance, shown in Figures 2 and 3, allows the equivalent output inductance to appear low without affecting the cell inductances.

An inversely coupled inductor is simply a interphase transformer (IPT) [6] without any leakage inductance. An IPT with separate cell inductances that represent the leakage would be equivalent to a coupled inductor system. Park and Kim [6] consider different construction techniques for IPTs.

Now that the cell inductances and output inductances can be adjusted independently, the magnetising currents can be kept very low.

The magnetising inductance can now be increased quite dramatically without increasing the volume of the core. This is because the magnetising inductance only needs to be rated to handle the flux generated by the magnetising current, not the output current. The limit to increasing magnetising inductance is that the window area still needs to fit the  $N$  turns with output current in them. Therefore the core still has to have a long path length. Other practicalities also get in the way of hugely increasing the magnetising inductance, mismatched average cell currents produce imperfect output current flux cancellation. These mismatches could be due to any number of factors. Some examples are differences in pulse width, cell resistance, mutual inductances and leakage inductances.

The inversely coupled converter offers a possible further decrease in transient response time. If mass and volume are of relatively little concern, as they are in VRMs for processors, the inversely coupled converter offers a method to have the full  $n^2$  reduction in transient response time without the  $n^2$  increase in cell current ripple percentage.

### III. RMS current calculation

Voltage averaging is a fundamental concept that may be applied to any inductive filter. When applied to parallel-interleaved converters it forms the basis of mathematical derivations that lead to the simplified equivalent models presented in Figures 2 and 3.

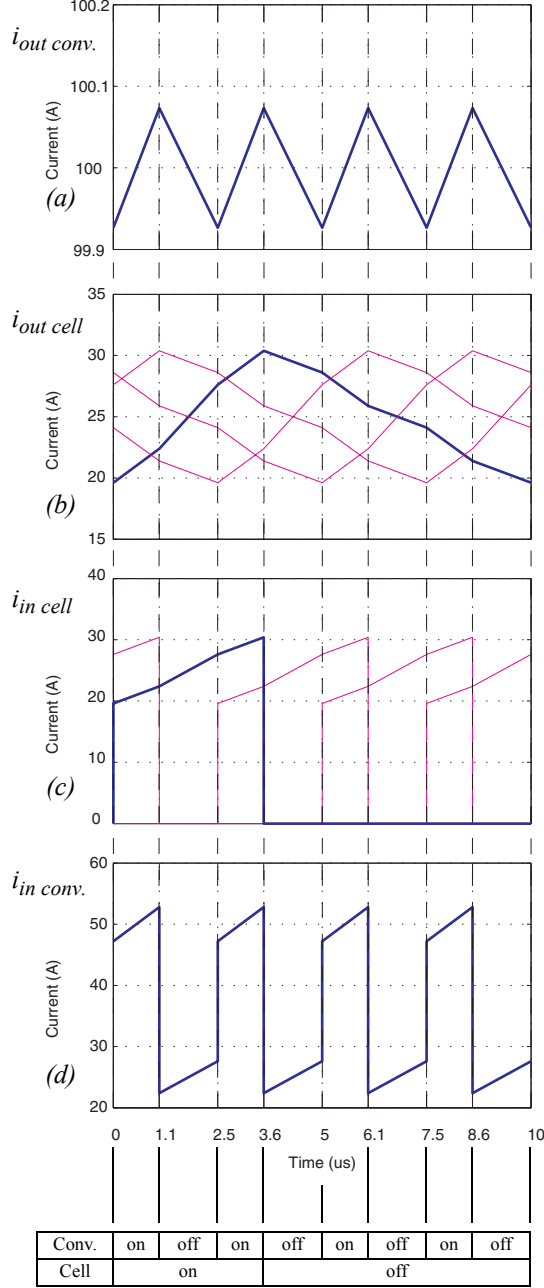


Figure 4 - Current waveforms of a 5-level direct coupled system with  $leakage = 1\mu H$ ,  $Mutual = 5\mu H$ , input voltage = 5V, output voltage 1.8V (Duty 36%) and output current = 100A. The switching frequency is 100kHz. The current waveforms are (a) converter output current, (b) cell output current, (c) cell input current and (d) converter input current.

The output current model reduces to a voltage source switching between the two averaged voltages and an equivalent inductance. Once the two output

current rate changes are known, voltage  $V_m$  is also known. Four different cell current rate changes are now easily calculated from the combination of the two  $V_{sI}$  values and the two  $V_m$  values. Modulo arithmetic is then used to calculate all the points needed to construct the cell and input current waveforms.

#### A. Output current waveform and RMS value

The output equivalent circuit shown in Figure 3 is extremely simple, being no different to a single buck converter. This leads to an output current waveform of Figure 4(a).

The voltage source of Figure 3 steps between the two closest voltage levels to the output voltage. It does this at the effective switching frequency  $f'_s = nf_s$ , period  $T'_s = T_s/n$  and with duty cycle  $D' = nD - \lfloor nD \rfloor$ . With  $\lfloor nD \rfloor$  being the  $nD$  rounded down to the closest whole number. The output current ripple is now quite easily calculated.

The converter on time is given by  $t'_{on} = D'T'_s$  and the converter off time is given by  $t'_{off} = T'_s - t'_{on}$ .

The converter source voltage when the converter is off is given by  $v_{s(off)} = (V_{in}/n)\lfloor nD \rfloor$  and the converter source voltage when the converter is on is given by  $v_{s(on)} = (V_{in}/n)(\lfloor nD \rfloor + 1)$ . The two different output current slopes are given in equation (2).

$$\begin{aligned} \dot{i}_{o(off)} &= \frac{v_{s(off)} - V_o}{\frac{L-M}{n} + M} \\ \dot{i}_{o(on)} &= \frac{v_{s(on)} - V_o}{\frac{L-M}{n} + M} \end{aligned} \quad (2)$$

If all the calculations are correct so far,  $\Delta i_{o(on)} = \dot{i}_{o(on)} \times t'_{on}$  equals  $-\Delta i_{o(off)} = \dot{i}_{o(off)} \times t'_{off}$ .

Given that  $I_o$  is the DC component of  $i_o$  the RMS current is given by equation (3).

$$i_{o(rms)} = I_o \sqrt{1 + \frac{1}{12} \left( \frac{\Delta i_{o(on)}}{I_o} \right)^2} \quad (3)$$

#### B. Cell current model

As was stated earlier there are four possible different slopes that comprise the cell current related to the two possible values of  $v_m$  and the two possible values of  $v_{sI}$ . These four different slopes can be seen in Figure 4(b), which is the plot of the cell current for a 4-cell (5-level) directly coupled converter.

It should be noted that below a duty cycle of  $1/n$  there are only three different slopes. This is because in this situation only one switch at a time can be on and this means that if the cell is on the converter must also be on. This situation also occurs at the other end of the duty cycle scale. When the duty cycle is above  $(n-1)/n$ , if the cell is off the converter must be off. In a three

level case there are only ever three different slopes in a cycle. The small table at the bottom of Figure 4 allows this phenomenon to be easily observed.

The equiangular displaced phases of interleaving means that a cell turns on every  $T_s'$  seconds, in the case of Figure 4 that is  $2.5\mu s$ . The same or different cell will turn off  $t_{on}' = D'T_s'$  seconds later. This gives a total of  $2n$  sections to the cell ripple current.

The first step in being able to create the above waveform is to calculate the number of times each type of slope segment occurs in a cycle. These values are given in equation (4).

$$\begin{aligned} n_{seg(on,on)} &= \lfloor nD \rfloor + 1 \\ n_{seg(on,off)} &= \lfloor nD \rfloor \\ n_{seg(off,on)} &= n - n_{seg(on,on)} \\ n_{seg(off,off)} &= n - n_{seg(on,off)} \end{aligned} \quad (4)$$

The number, length and position of each section of the cell ripple current shown in Figure 4(b) can now be found. To completely define the waveform the slope of each section must be found.

Equation (2) gives the two different values for the output current rate change, from these,  $v_m$  is quickly obtain by simply multiplying by  $M$ , giving equation (5).

$$\begin{aligned} v_{m(off)} &= Mi_{o(off)} + V_o \\ v_{m(on)} &= Mi_{o(on)} + V_o \end{aligned} \quad (5)$$

Equation (5) allows Figure 3 to be changed to assist with visualising the cell current waveform. The combination of switch A and B cause the four different slopes seen in Figure 4(b).

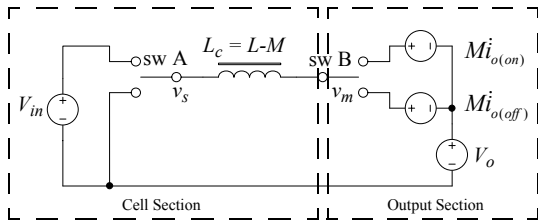


Figure 5 - Equivalent circuit for cell current.

Given  $v_m$  is now defined, equation (6) is a simple step from Figure 2.

$$\begin{aligned} i_{c1(on,on)} &= (V_{in} - v_{m(on)}) / (L - M) \\ i_{c1(on,off)} &= (V_{in} - v_{m(off)}) / (L - M) \\ i_{c1(off,on)} &= -v_{m(on)} / (L - M) \\ i_{c1(off,off)} &= -v_{m(off)} / (L - M) \end{aligned} \quad (6)$$

The change in current while the cell is on,  $\Delta i_{c1(on)}$ , is given by equation (7). The RMS cell current can be estimated by assuming that the current is triangular in

shape. This estimate of the RMS current is given in equation (8).

$$\begin{aligned} \Delta i_{c1(on)} &= \Delta i_{c1(on,on)} + \Delta i_{c1(on,off)} \\ \text{where } \Delta i_{c1(on,on)} &= n_{seg(on,on)} \times t'_{on} \times i_{c1(on,on)} \\ \text{and } \Delta i_{c1(on,off)} &= n_{seg(on,off)} \times t'_{off} \times i_{c1(on,off)} \\ \text{and } \Delta i_{c1(off,on)} &= n_{seg(off,on)} \times t'_{on} \times i_{c1(off,on)} \\ \text{and } \Delta i_{c1(off,off)} &= n_{seg(off,off)} \times t'_{off} \times i_{c1(off,off)} \end{aligned} \quad (7)$$

$$i_{c1(rms)} = \frac{1}{n} I_o \sqrt{1 + \frac{1}{12} \left( \frac{\Delta i_{c1(on)}}{\frac{1}{n} I_o} \right)^2} \quad (8)$$

The accuracy of equation (8) is worse when there is only a low number of levels. The accuracy is further reduced when the effective magnetising current is a lot higher than the output current. Figure 6 shows examples of (a) poor and (b) average accuracy.

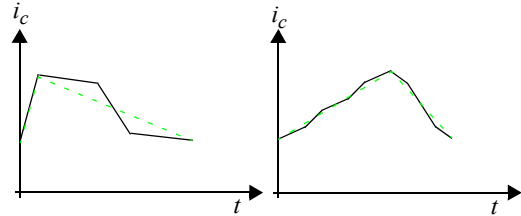


Figure 6 - Cases of cell current ripple, (a) 3-level with direct with low leakage (b) 5-level direct with the same leakage.

Absolute worst case is when Figure 6(a) tends towards a square wave and has no dc current. The square wave would have a RMS current of  $(1/2)\Delta i_{c1}$ , the triangular estimate would have a RMS current of  $(1/2)\sqrt{1/3}\Delta i_{c1}$  meaning that the estimate could be up to 42% wrong.

Alternatively, if it is only converters with low numbers of cells that can not be estimated this way, each of the  $2n$  points ( $I_1$  to  $I_{2n}$ ) of their cell output current waveform could quite easily be calculated and used with equation (9) to get the exact value for the cell RMS current. Equation (9) is derived from an equation for the RMS of a general piece wise waveform, given in Appendix A of [7].

$$i_{c1(rms)} = \sqrt{\frac{1}{3} \left[ \sum_{j=1}^{2n} I_j^2 + D' \left( \sum_{j=1}^n I_{2j-1} I_{2j} \right) + (1-D') \left( \sum_{j=1}^{n-1} I_{2j} I_{2j+1} + I_{2n} I_1 \right) \right]} \quad (9)$$

### C. Input current model

Only the cells that are on contribute to the input current. When the converter is off  $n_{i(off)}$  cells are on and all have a current rate change of  $i_{c1(on,off)}$  in each of them. When the converter is on  $n_{i(on)}$  cells are on and all have a current rate change of  $i_{c1(on,on)}$ .

For the first time the average output current features in a ripple current calculation. As can be seen from the circled example of Figure 7, when the average current during a segment is above  $I_o/n$  there is always a complementary segment that is the same amount below  $I_o/n$ . This therefore means that the summed average input current over any given time segment can be assumed to be  $n_i(I_o/n)$ .

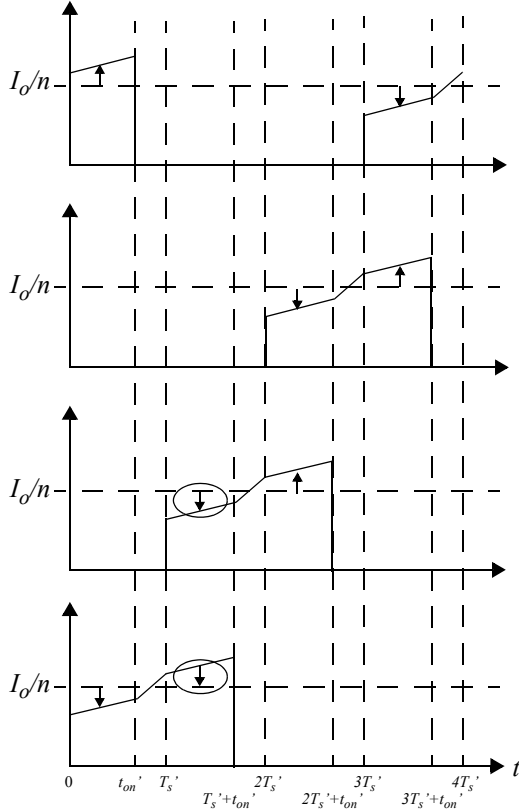


Figure 7 - Example of cell input current offsets cancelling.

To define the converter input current waveform of Figure 4(d), the average and change in current for the on and off times of the converter have to be found. These values are given in equation (10).

$$\begin{aligned}
 \Delta i_{i(off)} &= n_{i(off)} \times \dot{i}_{cl(on,off)} \times t'_{off} \\
 I_{i(off)} &= n_{i(off)} \times \frac{1}{n} I_o \\
 \Delta i_{i(on)} &= n_{i(on)} \times \dot{i}_{cl(on,on)} \times t'_{on} \\
 I_{i(on)} &= n_{i(on)} \times \frac{1}{n} I_o
 \end{aligned} \tag{10}$$

This results in a input current waveform shown in Figure 8 with points defined by equation (11).

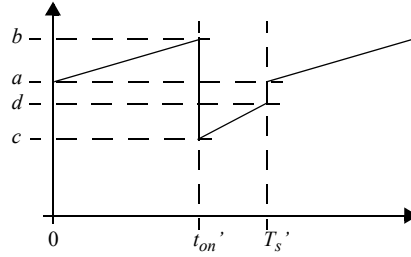


Figure 8 - The converter input current waveform.

$$\begin{aligned}
 a &= I_{i(on)} - \frac{1}{2} \Delta i_{i(on)}, & b &= I_{i(on)} + \frac{1}{2} \Delta i_{i(on)}, \\
 c &= I_{i(off)} - \frac{1}{2} \Delta i_{i(off)}, & d &= I_{i(off)} + \frac{1}{2} \Delta i_{i(off)}.
 \end{aligned} \tag{11}$$

The RMS input current can now be simply calculated using equation (12). To find the input capacitor ripple current the average input current  $I_{in} = DI_o$  should be taken from the two  $I_i$  values before using them in equation (12).

$$I_{rms} = \sqrt{D \times \left( I_{i(on)}^2 + \frac{1}{12} (\Delta i_{i(on)})^2 \right) + (1-D) \times \left( I_{i(off)}^2 + \frac{1}{12} (\Delta i_{i(off)})^2 \right)} \tag{12}$$

## IV. Conclusion

This paper proposed a new equivalent model for coupled systems that includes a multilevel voltage source. A procedure that allows calculation of the input, cell and output ripple currents by hand has also been proposed.

Consideration is also given to the application appropriateness of the different coupling types. The benefits of uncoupled interleaved converters were presented to allow a fair comparison to direct and inversely coupled systems.

It was noted that direct coupling was no different to simply adding a separate common inductance to a uncoupled system. The concept of using clamped zero voltage switching was also introduced as a method of benefiting for direct coupling.

Inversely coupled systems offered advantages in VRMs where best fast transient response and low output ripple voltage are needed. Inversely coupled systems allow the effective output inductance to reduce while increasing the effective cell inductance. This means that there is no limit to the number of levels that could be used in inversely coupled systems, whereas a uncoupled system in the same situation would end up with massive cell current ripple percentages.

Finally, a system allowing the calculation of input, cell and output current ripples is also proposed. This assists greatly with preliminary designs.

## Appendix

### A. Voltage averaging

The purpose of this section is to confirm the concept of voltage averaging. Starting with the coupled inductor equation (13), a mathematical expression describing the equivalent output circuit is derived, giving equation (14).

$$\begin{pmatrix} V_1 \\ V_2 \\ \vdots \\ V_n \end{pmatrix} = \begin{pmatrix} L & M & \cdots & M \\ M & L & \cdots & M \\ \vdots & \vdots & \ddots & \vdots \\ M & M & \cdots & L \end{pmatrix} \begin{pmatrix} i_1 \\ i_2 \\ \vdots \\ i_n \end{pmatrix} \quad (13)$$

$$V_1 = Li_1 + Mi_2 + \cdots + Mi_n \quad (\text{eq 1})$$

$$V_2 = Mi_1 + Li_2 + \cdots + Mi_n \quad (\text{eq 2})$$

$$\vdots$$

$$V_n = Mi_1 + Mi_2 + \cdots + Li_n \quad (\text{eq } n)$$

$$\sum_{k=1}^n (\text{eq } k) \Rightarrow$$

$$\sum_{k=1}^n V_k = (L + (n-1)M)i_1 + (L + (n-1)M)i_2 + \cdots + (L + (n-1)M)i_n$$

$$\sum_{k=1}^n (V_{in_k} - V_o) = (L + (n-1)M)(i_1 + i_2 + \cdots + i_n)$$

$$\sum_{k=1}^n V_{in_k} - nV_o = (L + (n-1)M)i_o$$

$$\frac{\sum_{k=1}^n V_{in_k}}{n} - V_o = \left( \frac{L}{n} + \frac{(n-1)M}{n} \right) i_o$$

$$\bar{V}_{in} - V_o = \left( \frac{L}{n} + \frac{(n-1)M}{n} \right) i_o = \left( \frac{L-M}{n} + M \right) i_o \quad (14)$$

### B. Equivalent Inductances

The purpose of this section is to confirm that  $L-M$  is the equivalent cell inductance  $L_c$  and  $M$  is the equivalent common output inductance  $L_o$  of Figure 2. Equation (15) is derived from the first line of the matrix equation (13). The same derivation holds for all lines of equation (13).

$$V_1 = Li_1 + M(i_2 + i_3 + \cdots + i_n)$$

$$V_{s1} - V_o = Li_1 + M(i_o - i_1)$$

$$V_{s1} - V_o = (L-M)i_1 + Mi_o \quad (15)$$

### C. Inversely coupled mutual inductance

The purpose of this section is to confirm that a inversely coupled system, shown in Figure 1(c), can be modelled using the coupled inductor equation (13) and hence modelled using the method presented in this paper. This process will also confirm that the mutual

inductance,  $M$ , for an inversely coupled inductor is in fact  $-L_m/(n-1)$ .

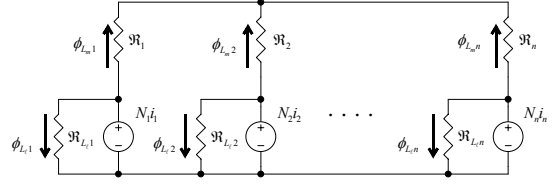


Figure 9 - Reluctance network for multi-leg inversely coupled inductor.

Starting with the magnetic circuit of an inversely coupled inductor, shown in Figure 9. By applying standard circuit theory and assuming that all the reluctances,  $\mathfrak{R}_i$ , are equal and all turns,  $N_i$ , are equal, equations (16) and (17) can be written.

$$Ni_1 - \phi_{L_m} \mathfrak{R} = Ni_2 - \phi_{L_m} \mathfrak{R} = \cdots = Ni_n - \phi_{L_m} \mathfrak{R} \quad (16)$$

$$0 = \phi_{L_m1} + \phi_{L_m2} + \cdots + \phi_{L_mn} \quad (17)$$

Using equation (16) to express all the fluxes in terms of  $\phi_{L_m1}$ , equation (18) is obtained.

$$\begin{aligned} \phi_{L_m2} &= \frac{Ni_2 - (Ni_1 - \phi_{L_m1} \mathfrak{R})}{\mathfrak{R}} = \frac{Ni_2 - Ni_1 + \phi_{L_m1} \mathfrak{R}}{\mathfrak{R}} \\ \phi_{L_m3} &= \frac{Ni_3 - Ni_1 + \phi_{L_m1} \mathfrak{R}}{\mathfrak{R}} \\ &\vdots \\ \phi_{L_mn} &= \frac{Ni_n - Ni_1 + \phi_{L_m1} \mathfrak{R}}{\mathfrak{R}} \end{aligned} \quad (18)$$

Equations (18) can now be substituted into equation (17) resulting in equation (19), which gives  $\phi_{L_m1}$ .

$$\begin{aligned} 0 &= \phi_{L_m1} + \phi_{L_m2} + \cdots + \phi_{L_mn} \\ &= \phi_{L_m1} + \frac{Ni_2 - Ni_1 + \phi_{L_m1} \mathfrak{R}}{\mathfrak{R}} + \frac{Ni_3 - Ni_1 + \phi_{L_m1} \mathfrak{R}}{\mathfrak{R}} + \\ &\quad \cdots + \frac{Ni_n - Ni_1 + \phi_{L_m1} \mathfrak{R}}{\mathfrak{R}} \\ &= \phi_{L_m1} \mathfrak{R} + Ni_2 - Ni_1 + \phi_{L_m1} \mathfrak{R} + Ni_3 - Ni_1 + \phi_{L_m1} \mathfrak{R} + \\ &\quad \cdots + Ni_n - Ni_1 + \phi_{L_m1} \mathfrak{R} \\ &= n\phi_{L_m1} \mathfrak{R} - (n-1)Ni_1 + \sum_{i=2}^n Ni_i \\ n\phi_{L_m1} \mathfrak{R} &= (n-1)Ni_1 - \sum_{i=2}^n Ni_i \\ &\quad (n-1)Ni_1 - \sum_{i=2}^n Ni_i \\ \phi_{L_m1} &= \frac{(n-1)Ni_1 - \sum_{i=2}^n Ni_i}{n\mathfrak{R}} \end{aligned} \quad (19)$$

Adding the leakage term to equation (19) gives equation (20), which gives the total flux generated by coil one,  $\phi_{L1}$ .

$$\phi_{L1} = \frac{1}{n\mathfrak{R}} [(n-1)Ni_1 - Ni_2 - Ni_3 - \cdots - Ni_n] + \frac{Ni_1}{\mathfrak{R}_{L_i}} \quad (20)$$

Differentiating equation (20) with respect to time and applying Faraday's law gives equation (21).

$$\begin{aligned} \frac{d\phi_{l1}}{dt} &= \frac{1}{n\Re} [(n-1)Ni_1 - Ni_2 - Ni_3 - \dots - Ni_n] + \frac{Ni_1}{\Re_{L_t}} \\ N_1 \frac{d\phi_{l1}}{dt} &= \frac{1}{n\Re} [(n-1)N^2i_1 - N^2i_2 - N^2i_3 - \dots - N^2i_n] + \frac{N^2i_1}{\Re_{L_t}} \\ V_1 &= \left( \frac{N^2}{\Re_{L_t}} + \frac{N^2}{n\Re} \right) i_1 - \frac{N^2}{n\Re} i_2 - \frac{N^2}{n\Re} i_3 - \dots - \frac{N^2}{n\Re} i_n \end{aligned} \quad (21)$$

Equation (21) can be seen to fit the form of equation (13){eq 1} exactly, showing the inversely coupled system also complies to the coupled inductor equation (13). This allows equations (22) to be written.

$$\begin{aligned} L_t &= \frac{N^2}{\Re_{L_t}} \\ L_m &= (n-1) \frac{N^2}{n\Re} \\ M &= -\frac{N^2}{n\Re} \end{aligned} \quad (22)$$

The inductance values of equations (22) gives equation (23), the inversely coupled mutual inductance in terms of magnetising inductance.

$$M = -\frac{L_m}{(n-1)} \quad (23)$$

## References

- [1] P-L. Wong, P. Xu, B. Yang and F. C. Lee, "Performance Improvements of Interleaving VRMs with Coupling Inductors", IEEE Transactions on Power Electronics, vol. 16, no. 4, 2001, pp 499-507.
- [2] P-L. Wong, F. C. Lee, X. Jia, D. Wyk, "A Novel Modelling Concept for Multi-coupling Core Structures", IEEE Applied Power Electronics Conference and Exposition, 4-8 March, 2001, vol. 1, pp 102-108.
- [3] J. Li, C. R. Sullivan and A. Schultz, "Coupled-Inductor Design Optimization for Fast-Response Low-Voltage DC-DC Converters", IEEE Applied Power Electronics Conference and Exposition, 10-14 March, 2002, vol. 2, pp 817-823.
- [4] J. Czogalla, J. Li, C. R. Sullivan, "Automotive Application of Multi-Phase Coupled-Inductor DC-DC Converter", IEEE Industry Applications Conference, 12-16 Oct., 2003, vol. 3, pp 1524-1529.
- [5] S. Chandrasekaran, V. Mehrotra and J. Sun, "A New Matrix Integrated Magnetics (MIM) Structure for Low Voltage, High Current DC-DC Converters", IEEE Power Electronics Specialists Conference, 23-27 June, 2002, vol. 3, pp 1230-1235.
- [6] I. G. Park and S. I. Kim, "Modeling and Analysis of Multi-Interphase Transformers for Connecting Power Converters in Parallel", IEEE Power Electronics Specialists Conference, 22-27 June, 1997, vol. 2, pp 1164-1170.
- [7] R. W. Erickson and D. Maksimovic, "Fundamentals of Power Electronics - Second Edition", 2001, Kluwer Academic Publishers.